

PAPER • OPEN ACCESS

Natural Oscillations of Welded Steel Beams in the Span Structures of Conveyor Galleries

To cite this article: V Volkova and I Smolii 2015 *IOP Conf. Ser.: Mater. Sci. Eng.* **96** 012071

View the [article online](#) for updates and enhancements.

You may also like

- [Belt conveyor speed detection based on fiber-optic Sagnac interferometer vibration sensor](#)

Yaru Hou, Pingjuan Niu, Jia Shi et al.

- [New approaches to the development of hybrid nanocomposites: from structural materials to high-tech applications](#)

V A Gerasin, E M Antipov, V V Karbushev et al.

- [Research on a system for the diagnosis and localization of conveyor belt deviations in belt conveyors](#)

Lei Wu, Junxia Li, Hongyu Zhang et al.



DISCOVER
how sustainability
intersects with
electrochemistry & solid
state science research

Natural Oscillations of Welded Steel Beams in the Span Structures of Conveyor Galleries

V Volkova^{1,2} and I Smolii¹

¹SHEI “National Mining University”, Department of Construction, Geotechnics and Geomechanics, 19 Karla Marksa Ave., Dnipropetrovsk 49000, Ukraine

E-mail: sebrle@bk.ru

Abstract. This article presents the results of numerical simulation of dynamic behaviour of welded metal beams in conveyor galleries. Investigations were carried out for the beams having symmetrical cross-sections and evenly-spaced transversal ribs with various spacing between the ribs in different beams. The regularities of changes in the vibration mode shapes depending on the beam geometric characteristics have been investigated.

1. Introduction

Belt conveyors have gained widespread acceptance for charging materials along the belt-conveyor trestles into the blast furnaces in the metallurgical coal-preparation and ore-dressing plants, for transporting extracted materials onto the surface in the open pit and underground mining, in the building and construction sector as well as in other industries. Belt conveyors are installed in adequate buildings and premises or in purpose-built galleries between these structures [1].

The experience gained in the 70-year period of industrial operation of the galleries in Ukraine proves that these structures belong to the class of facilities of the first criticality level. High damage rates in the galleries stem from the concurrent effects of a number of adverse factors, including dynamic loads [2].

Articulated and thin-walled beams, parallel-chord trusses, rectangular and circular cylindrical shells as well as other types of structural elements can be used as span bearing structures. From the point of view of cost saving and operating economy, the application of beam bearing structures is rational for the spans up to 30 m in length, while for the spans ranging from 24 m to 42 m it is recommended to use lattice girders as the load-bearing structures, particularly trusses. Shells may also be used as the load-bearing structures in the conveyor galleries with the spans exceeding 30 m in length [2]. They have higher reliability and require less operating expenditures as compared to trusses. Depending on

² To whom any correspondence should be addressed.



technological requirements, the span structures of conveyor galleries can be installed straight or inclined (10-15°) [6].

2. The object of research

The objects of this research are conveyor gallery span structures. These structures are the facilities of the first criticality level. With an aim to ensure the best reliability, strength and stability of span structures at all stages of their manufacturing, transportation and erection, the up-to-date Regulations and Standards of construction practices provide guidance to the selection of geometrical parameters and stiffness characteristics for the span structures.

In the real-world beam structural systems, a number of initial imperfections of the elements can be found, in particular, bent portions, curvature bending under transverse loads, and other defects. For this reason, the limit ratio of b_f/t_f as recommended in the Standards is slightly less than the value obtained on the basis of an idealized design scheme [3].

According to the State Standards and Norms for construction in Ukraine (DBN V.2.6-163: 2010), the conventional boundary slenderness parameters should be set as $\bar{\lambda}_{uf} = 0,36 + 0,1\bar{\lambda}$, for the beam chords and $\bar{\lambda}_{uw} = 1,30 + 0,15\bar{\lambda}^2$ for the web. In this case, the parameter $\bar{\lambda}$ is conventional slenderness of the structural framing, which is determined taking into account the overall stability of the system under the action of the central compression force [4].

Technological loads acting on the structural elements of conveyor galleries are dynamic in nature, due to induced vibrations of the conveyor belt transporting bulk material at various stages of operation. Due to this fact, investigations into dynamic characteristics of the span structures of conveyor galleries are of great significance.

Formerly, when calculating conveyor gallery structures, the most commonly used method was based on the flat cross-section hypothesis [10]. However, for dynamic behaviour of beams in the span structures, such approach is rather approximate. The models suggested by Timoshenko and Vlasov have also found a wide application [7].

3. The method of investigations

Simulation was performed for simply supported pin-ended beams. The results were obtained with the use of the SCAD software package and implementation of Lanczos method for dynamic analysis [8]. Rectangular finite element mesh was used in research. The finite elements represented the plates of 100×100 mm in size and 20 – 40 mm thick [12]. According to the standards, it is recommended to analyze from 3 to 5 principal modes of vibration. In order to avoid the building-up of errors in integration, simulation was carried out for 10 modes of vibration. In further investigations the first 5 modes were used. The results obtained were compared to available approximate solutions [9].

The computation was performed using the finite element method with the SCAD PC Programming Software. The numerical analysis was performed in the computation of the beams with the specified geometrical characteristics. The reduced values of slenderness of the beam webs varied within the range of $\bar{\lambda}_w = 2.5 \div 13$ and the slenderness ratios of the beam chords varied within the particular range of $b_f/t_f = 10 \div 40$.

The boundary conditions corresponded to a hinged structure. Dimensions of the beam cross sections were chosen in accordance with the recommendations in “The Handbook on Conveyor Gallery Designs”, the Supplement to SNiP (Local Building Requirements) 2.09.03-85”. The data were obtained for the I-section welded beam of the span length of 12 m. The web of beam was connected with the flanges via filled welds. Disposition, effective throat thickness and effective length of welds

were chosen in accordance with the recommendations of [13]. The cross-sectional view of the beam is shown in figure 1.

The finite elements used in the simulations represented “four-node rectangular plates” (FE-analysis 13), i.e. the plate members subjected to bending and lying in the plane XOY. The finite elements of this kind are generally useful in case of uniform thickness materials. In each node of these finite elements, three degrees of freedom were defined, namely: w - vertical displacement (sagging) and also UX and UY – the angles of rotation about the axes X and Y , respectively [11]. The control points were chosen at equal intervals along the top and bottom flanges of the beam, as well as on the web. Displacements were controlled in the nodes of the finite elements. The numerical designation of the nodes for this computation scheme is shown in figure 2.

In the theory of the finite element method, a lot of attention is paid to the problem of convergence, i.e. the asymptotic behaviour of the accuracy estimates of the obtained approximate solution with the

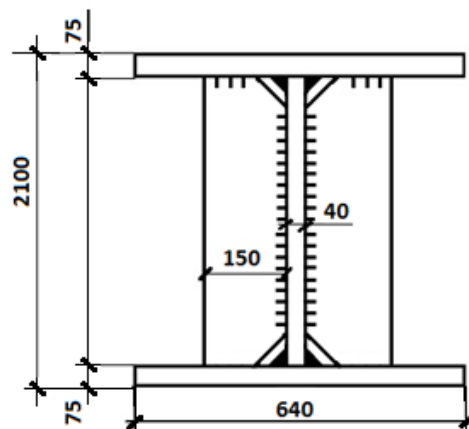


Figure 1. Cross-sectional view of the beam.

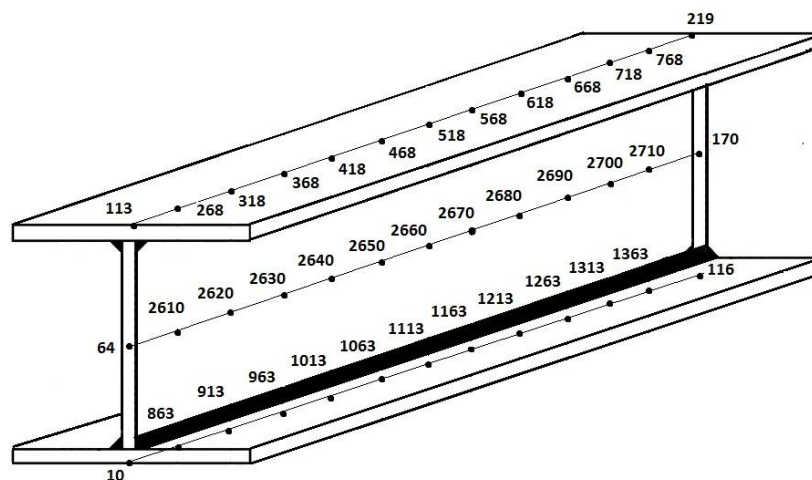


Figure 2. The numerical designation of the nodes for the computation scheme.

unlimited thickening of the finite element mesh. Proceeding from the results of the assessment of convergence of both the compatible finite elements and the incompatible ones, convergence of the given finite elements can be estimated. The spacings and density of the finite element mesh were chosen in accordance with the required accuracy of the approximate solution and also taking into account an uncertain error in the determination of stresses and deformations. According to the estimates given in the paper [5], the rates of convergence of the computing procedures for FE No. 13 came to 2 parameters for displacements, 2 parameters for moments and 1 parameter for transverse forces.

4. Analysis of the results obtained

Based on the results of the calculation, the following regularities of changes in the vibration mode shapes were determined for various reduced flexural capacities of the beam web and beam chord. In the tested slenderness range of the web $\bar{\lambda}_w = 2.5 \div 5.5$ and that of the beam flanges $b_f/t_f = 10 \div 40$, the beams with the slenderness values of $\bar{\lambda}_w = 2.5$ and $\bar{\lambda}_w = 3.2$ belong to the beams with the rigid web and those with the slenderness value of $\bar{\lambda}_w = 5.5$ are the beams with the flexible web. The mode shapes for flanges are given in figure 3 ($\bar{\lambda}_w = 2.5$), figure 4 ($\bar{\lambda}_w = 3.2$), figure 5 ($\bar{\lambda}_w = 5.5$).

The first type of the vibration mode shapes in the beam flanges corresponded exclusively to node free mode shapes. The vibration phase was constant. A single shift of the vibration phase was revealed in the transition of the ratio b_f/t_f from value 10 to value 20. The effects of the slenderness

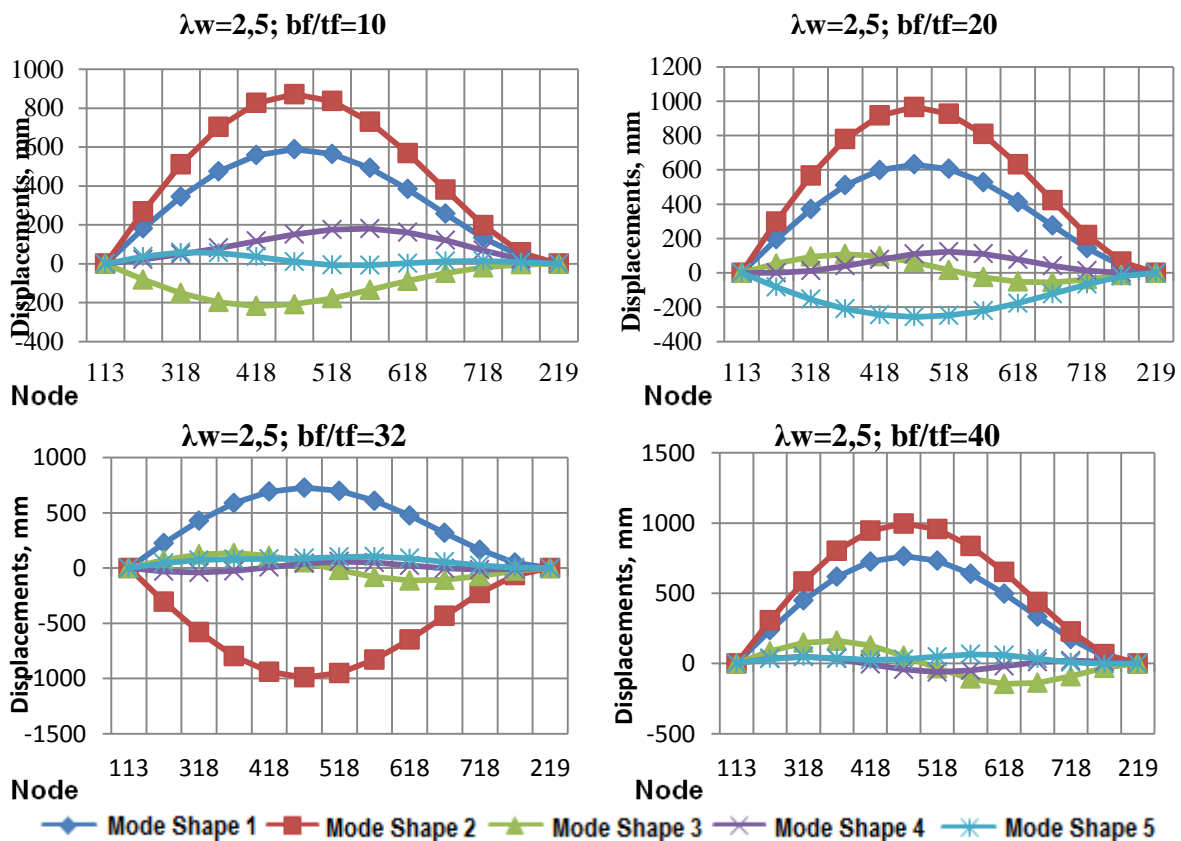


Figure 3. Vibration mode shapes in the beam flanges $\bar{\lambda}_w = 2.5$.

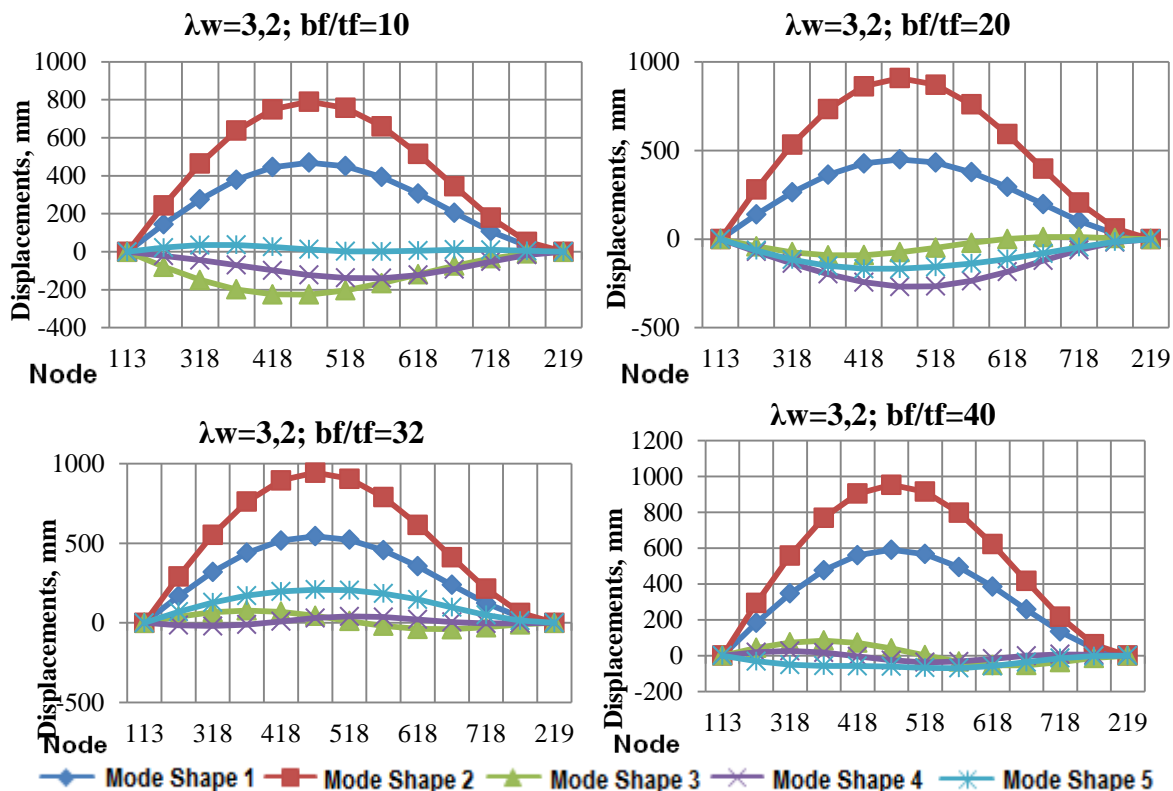


Figure 4. Vibration mode shapes in the beam flanges $\bar{\lambda}_w = 3.2$.

characteristics of the beam flanges and webs upon the vibration mode shapes of the second type are of the following nature. The beams demonstrated a node free mode shapes of vibrations. The shifts of the vibration phases were observed with the value of $\bar{\lambda}_w = 2.5$ in the transition of the ratio b_f/t_f from value 20 to value 32 and from value 32 to value 40. The shifts of the vibration phase were detected with the value $\bar{\lambda}_w = 5.5$ in the transition of the ratio b_f/t_f from value 10 to value 20. When the ratio b_f/t_f changed from value 20 to value 32, the transition from the node free vibration mode shapes to the single-node modes occurred.

The vibration mode shapes of the third type changed from the node free vibration mode shapes to the single-node ones in the transition of the ratio b_f/t_f from value 10 to value 20. In the transition of the ratio values of b_f/t_f from 20 to 32 with the parameter $\bar{\lambda}_w = 5.5$, the node free vibration mode shapes transformed into the two-node modes.

In the fourth type of vibration mode shapes, with the web slenderness reduced value $\bar{\lambda}_w = 2.5$, the transition of the vibrations from the node free modes into the single-node modes was observed when the ratio values of b_f/t_f changed from 10 to 20, but when the ratio values of b_f/t_f changed from 20 to 32, the single-node modes transformed into the two-node mode shapes. At the same time, the transition from the node free mode shapes to the two-node modes took place when the ratio values b_f/t_f changed from 20 to 32 and the value $\bar{\lambda}_w = 3.2$. The node free mode shapes are characteristic only for the value $\bar{\lambda}_w = 5.5$. Phase shifts were observed in both cases of transition of the ratio b_f/t_f from value 10 to value 20 and from value 20 to value 32.

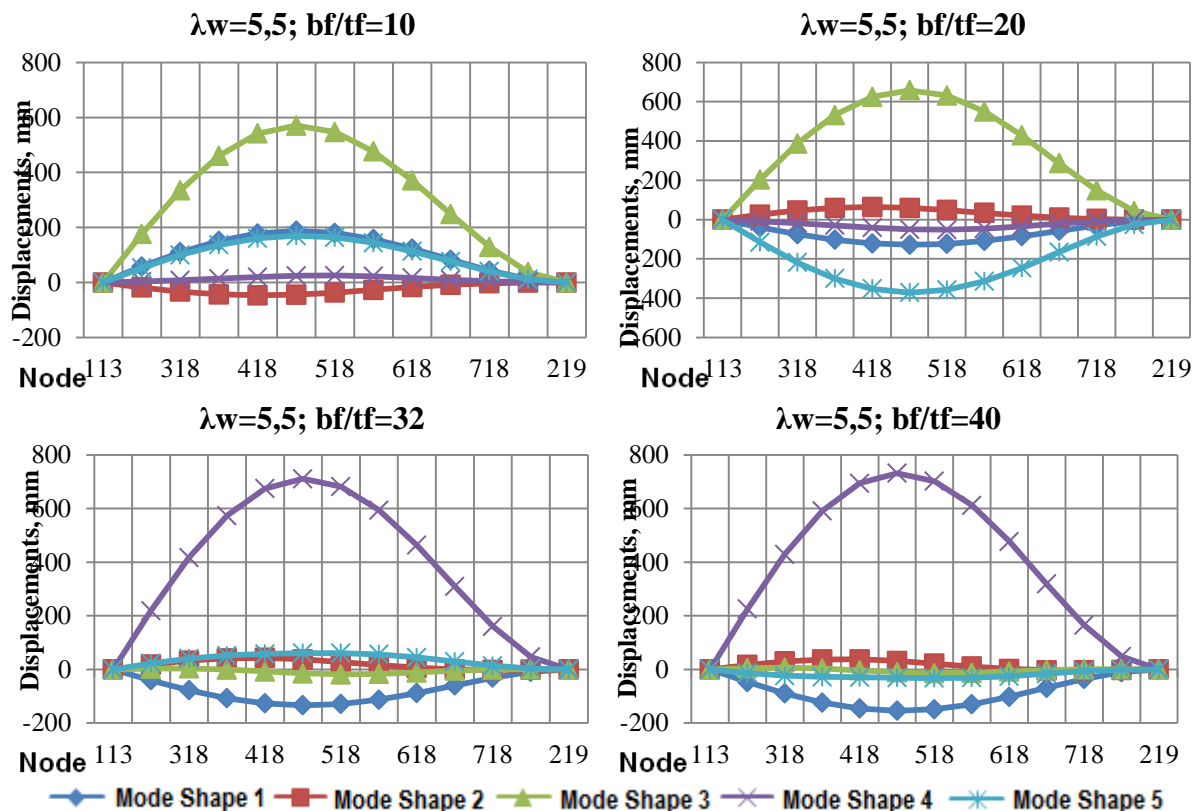


Figure 5. Vibration mode shapes in the beam flanges $\bar{\lambda}_w=5.5$.

The following changes are peculiar to the fifth type of the vibration mode shapes. With $\bar{\lambda}_w = 2.5$, the two-node mode shapes are typical for the value $b_f/t_f = 10$, while the node free modes are characteristic of the ratios $b_f/t_f = 20$ and $b_f/t_f = 32$. Only the node free vibration modes were revealed with $\bar{\lambda}_w = 3.2$ and $\bar{\lambda}_w = 5.5$, at that, with the value $\bar{\lambda}_w = 5.5$, phase shifts took place in the whole range of changes of the ratio values $b_f/t_f = 10 \div 40$.

The following regularities were revealed in the vibrations of the beam web. The mode shapes for the web are given in figure 6 ($\bar{\lambda}_w = 2.5$), figure 7 ($\bar{\lambda}_w = 3.2$), figure 8 ($\bar{\lambda}_w = 5.5$). The node free mode shapes corresponded to the first type of vibrations. With the value $\bar{\lambda}_w = 5.5$, phase shifts in vibrations occurred in the transition of the ratio b_f/t_f from value 10 to value 20.

At the same time, the node free mode shapes represented the second type of vibration modes. The single-node mode shapes are characteristic of the value $\bar{\lambda}_w = 5.5$, and phase shifts were detected when the ratios of b_f/t_f changed from value 10 to value 20.

The single-node mode shapes were characteristic of the third type of vibrations. Phase shifts were revealed with the value $\bar{\lambda}_w = 2.5$ in the transition of the ratio b_f/t_f from value 10 to value 20, and with the values of $\bar{\lambda}_w = 3.2$ and $\bar{\lambda}_w = 6$, phase shifts took place in the transition of the ratio b_f/t_f from value 20 to value 32. With the value $\bar{\lambda}_w = 5.5$, the transition from the node free mode shapes to the two-node vibration modes occurred when the ratio b_f/t_f changed from value 20 to value 32.

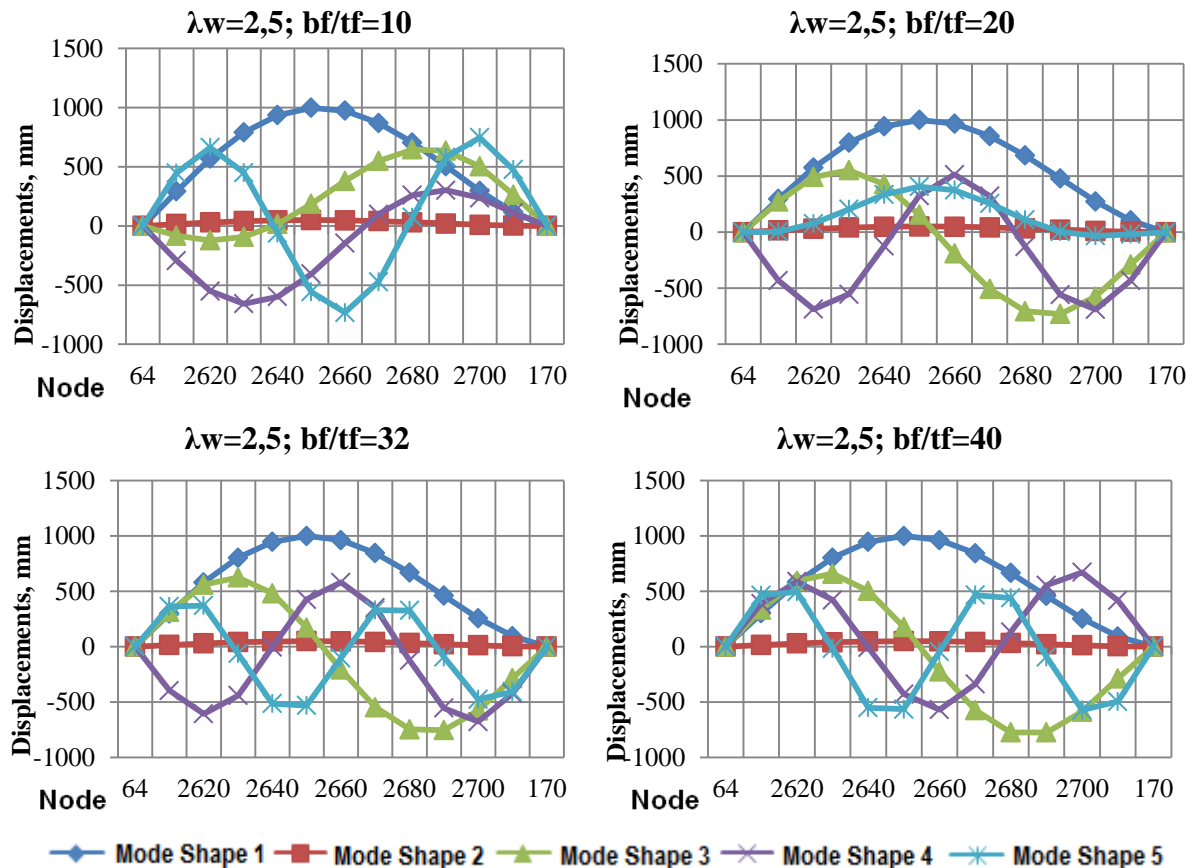


Figure 6. Vibration mode shapes in the beam web $\bar{\lambda}_w = 2.5$.

The transition of the vibrations from the single-node modes into the two-node modes was observed when the ratio b_f/t_f changed from value 10 to value 20. With the same values of $\bar{\lambda}_w$, phase shifts were revealed when the ratio b_f/t_f changed from value 32 to value 40. With the value $\bar{\lambda}_w = 5.5$, the two-node vibration modes transformed into the node free modes in the transition of the ratio b_f/t_f from value 20 to value 32, and phase shifts were detected when the ratio b_f/t_f changed from value 10 to value 20.

The changes of the $\overline{\lambda_w}$ and b_f/t_f parameters have more complex effects on the fifth type of the beam web mode shapes. With the value of $\overline{\lambda_w}=2.5$, during the transition of the ratio b_f/t_f from value 10 to value 20 and when the ratio b_f/t_f changes from value 20 to value 32, the single-node mode shapes passed into the two-node vibration modes; and when the values of the ratio b_f/t_f ran from 32 to 40, phase shifts were detected. At the same time, with the value of $\overline{\lambda_w}=3.2$, the two-node vibration mode shapes evolve into the three-node modes when the ratio b_f/t_f was passing from value 20 to value 32, while the vibration phase shifts were observed in both cases – when the ratio values of b_f/t_f were going from 10 to 20 and from 32 to 40. With the value of $\overline{\lambda_w}=5.5$, the three-node modes with the phase shifts were revealed in the whole range of the varying parameter $b_f/t_f=10\div 40$.

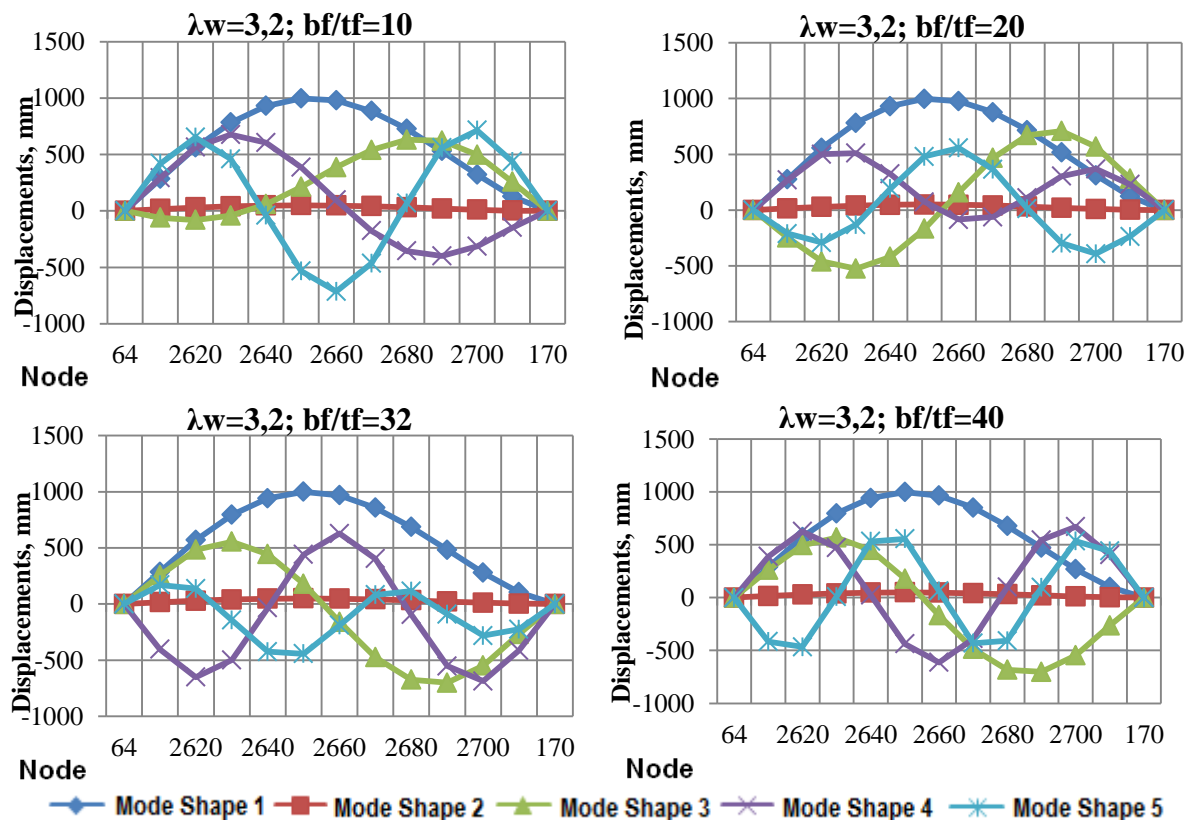


Figure 7. Mode shapes in the beam web $\overline{\lambda_w}=3.2$.

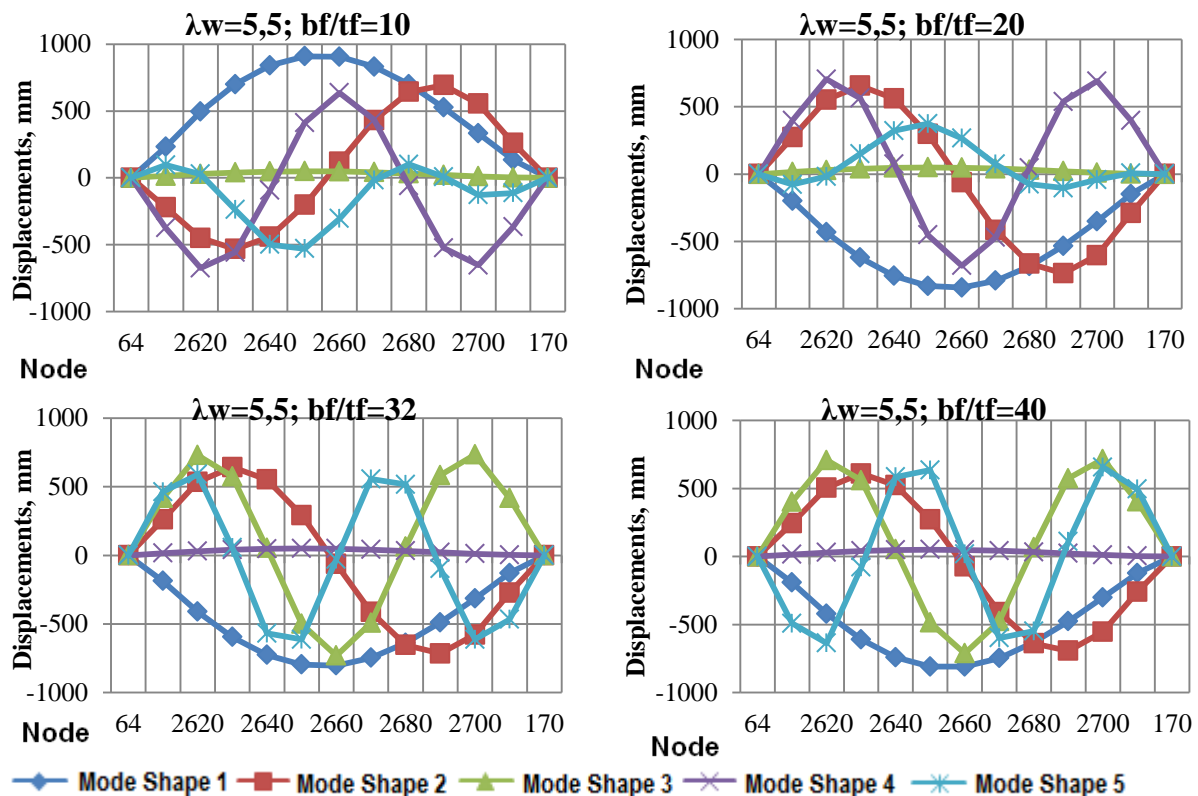


Figure 8. Mode shapes in the beam web $\bar{\lambda}_w=5.5$.

5. Conclusions

Free oscillations of the system are a type of motion, which is realized in the system in the absence of any external influence or power impact from the outside. The results of the analysis of various modes of forced vibration mode shapes enable to reveal the internal dynamic characteristics. Based on these characteristics, it is feasible to predict the response of the structure to the influence of various external factors.

With the higher-level slenderness of the beam chords, the vibration amplitudes of the two lower-order mode shapes increase. The natural frequencies in the beams with the flexible webs decrease when the slenderness of the beam chord increases. The emergence of the two- and four-node vibration mode shapes was observed when the slenderness of the beam flange increased. With the higher-level slenderness of the beam webs and chords, the appearance of additional nodes in the mode shapes was revealed.

6. References

- [1] Gordeyev V N, Lantukh-Lyashenko A I, Pashinsky V A, Perel'muter A V, Pichugin S F 2007 *Loads and Effects on Buildings and Structures* (Moscow: Publishing House of Association of Building Universities)
- [2] Gorev V V 2002 *Metal Structures. Volume 3, Special Designs and Constructions* (Moscow: High School Publishing House)
- [3] Gorev V V 2002 *Metal Structures. Volume 1, Structural Elements* (Moscow: High School Publishing House)
- [4] *The State Standards and Norms for Construction in Ukraine (DBN V.2.6-163: 2010), Steel Structures* (Kiev: Minregionbud Publishing House of the Ministry of Regional Development, Construction and Housing and Communal Services of Ukraine)
- [5] Karpilovsky V S, Kriksunov E Z 2003 *CAD System for Users* (Kyiv)
- [6] *SNiP 2.09.03-85, Construction Rules and Regulations for Industrial Enterprises* (The USSR State Committee for Construction)
- [7] Soltani M, Asgarian B, Mohri F 2014 *Finite Element Method for Stability and Free Vibration Analyses of Non-prismatic Thin-walled Beams* (Thin Walled Structures vol. 82) pp 245–261
- [8] Fialko S 2007 The Lanczos method of displacements as applied for the seismic analysis of structures *CADmaster Magazine* **5** 102–105
- [9] Perel'muter A 2014 *Discourse on Construction Mechanics Scientific Edition* (Moscow: SCAD Soft).
- [10] Perel'muter A, Slivker V 2002 *Computational Models of Structures and Feasibility of their Analysis Scientific Edition* (Kiev: Stal Publishing House)
- [11] Bazhenov V A, Perel'muter A V, Shishov OV 2009 *Structural Mechanics. Computer Technologies* (Kiev: Karavela Publishing House)
- [12] Zinkevich O K 1975 *The Finite Element Method in Engineering* (Moscow: Mir Publishing House)
- [13] *EN 1993-1-8 2005: Eurocode 3: Design of Steel Structures - Part 1-8: Design of Joints* (Authority: The European Union Per Regulation 305/2011, Directive 98/34/EC, Directive 2004/18/EC) pp 38–50